

# The P2 nucleic acid binding protein of sugarcane bacilliform virus is a viral pathogenic factor (#91543)

1

First submission

## Guidance from your Editor

Please submit by **14 Dec 2023** for the benefit of the authors (and your token reward) .



### Structure and Criteria

Please read the 'Structure and Criteria' page for general guidance.



### Custom checks

Make sure you include the custom checks shown below, in your review.



### Raw data check

Review the raw data.



### Image check

Check that figures and images have not been inappropriately manipulated.

If this article is published your review will be made public. You can choose whether to sign your review. If uploading a PDF please remove any identifiable information (if you want to remain anonymous).

## Files

Download and review all files from the [materials page](#).

9 Figure file(s)

3 Table file(s)

10 Raw data file(s)

1 Other file(s)

## ! Custom checks

### DNA data checks

- ! Have you checked the authors [data deposition statement](#)?
- ! Can you access the deposited data?
- ! Has the data been deposited correctly?
- ! Is the deposition information noted in the manuscript?




# Structure and Criteria

---

## Structure your review

The review form is divided into 5 sections. Please consider these when composing your review:

1. BASIC REPORTING
2. EXPERIMENTAL DESIGN
3. VALIDITY OF THE FINDINGS
4. General comments
5. Confidential notes to the editor






 You can also annotate this PDF and upload it as part of your review

When ready [submit online](#).





## Editorial Criteria

Use these criteria points to structure your review. The full detailed editorial criteria is on your [guidance page](#).




### BASIC REPORTING

-  Clear, unambiguous, professional English language used throughout.
-  Intro & background to show context. Literature well referenced & relevant.
-  Structure conforms to [Peerj standards](#), discipline norm, or improved for clarity.
-  Figures are relevant, high quality, well labelled & described.
-  Raw data supplied (see [Peerj policy](#)).

### EXPERIMENTAL DESIGN

-  Original primary research within [Scope of the journal](#).
-  Research question well defined, relevant & meaningful. It is stated how the research fills an identified knowledge gap.
-  Rigorous investigation performed to a high technical & ethical standard.
-  Methods described with sufficient detail & information to replicate.

### VALIDITY OF THE FINDINGS

-  Impact and novelty not assessed. *Meaningful* replication encouraged where rationale & benefit to literature is clearly stated.
-  All underlying data have been provided; they are robust, statistically sound, & controlled.
-  Conclusions are well stated, linked to original research question & limited to supporting results.



The best reviewers use these techniques

## Tip

## Example

**Support criticisms with evidence from the text or from other sources**

*Smith et al (J of Methodology, 2005, V3, pp 123) have shown that the analysis you use in Lines 241-250 is not the most appropriate for this situation. Please explain why you used this method.*

**Give specific suggestions on how to improve the manuscript**

*Your introduction needs more detail. I suggest that you improve the description at lines 57- 86 to provide more justification for your study (specifically, you should expand upon the knowledge gap being filled).*

**Comment on language and grammar issues**

*The English language should be improved to ensure that an international audience can clearly understand your text. Some examples where the language could be improved include lines 23, 77, 121, 128 - the current phrasing makes comprehension difficult. I suggest you have a colleague who is proficient in English and familiar with the subject matter review your manuscript, or contact a professional editing service.*

**Organize by importance of the issues, and number your points**

1. Your most important issue
2. The next most important item
3. ...
4. The least important points

**Please provide constructive criticism, and avoid personal opinions**

*I thank you for providing the raw data, however your supplemental files need more descriptive metadata identifiers to be useful to future readers. Although your results are compelling, the data analysis should be improved in the following ways: AA, BB, CC*

**Comment on strengths (as well as weaknesses) of the manuscript**

*I commend the authors for their extensive data set, compiled over many years of detailed fieldwork. In addition, the manuscript is clearly written in professional, unambiguous language. If there is a weakness, it is in the statistical analysis (as I have noted above) which should be improved upon before Acceptance.*

# The P2 nucleic acid binding protein of sugarcane bacilliform virus is a viral pathogenic factor

Xiongbiao Xu<sup>Corresp., Equal first author, 1</sup>, Yinian Lou<sup>Equal first author, 1</sup>, Kaili Liang<sup>1</sup>, Jingying Liu<sup>1</sup>, Zhiyuan Wang<sup>1</sup>, Baoshan Chen<sup>1</sup>, Wenlan Li<sup>2</sup>

<sup>1</sup> State Key Laboratory for Conservation and Utilization of Subtropical Agro-bioresources, Guangxi key Laboratory of Sugarcane biology, College of Agriculture, Guangxi University, Nanning, China

<sup>2</sup> College of Life Science and Technology, Guangxi University, Nanning, Guangxi, China

Corresponding Author: Xiongbiao Xu  
Email address: xiongbiaox@gxu.edu.cn

**Background.** *Saccharum spp.* is the major source of sugar and plays significant roles in global renewable bioenergy. Sugarcane bacilliform virus (SCBV) is one of the most important viruses infecting sugarcane, causing severe yield losses and quality degradation. It is of great significance to reveal the pathogenesis of SCBV and resistance breeding. However, little is known about the viral virulence factors or RNA silencing suppressors and the molecular mechanism of pathogenesis.

**Methods.** To systematically investigate the functions of the unknown protein P2 encoded by SCBV ORF2. Phylogenetic analysis was implemented to infer the evolutionary relationship between the P2 of SCBV and other badnaviruses. The precise subcellular localization of P2 was verified in the transient infiltrated *Nicotiana benthamiana* epidermal mesophyll cells and protoplasts by using the Laser scanning confocal microscope (LSCM). The post-transcriptional gene silencing (PTGS) and transcriptional gene silencing (TGS) RNA silencing suppressor activity of P2 was analysed, respectively. And the probable mechanism of P2 on repressing DNA methylation was verified by restriction digestion and RT-qPCR. To explore the pathogenicity of P2, a potato virus X-based viral vector was used to heterologously express SCBV P2, and the consequent H<sub>2</sub>O<sub>2</sub> accumulation was detected by 3,3'-diaminobenzidine (DAB) staining method.

**Results.** Phylogenetic analysis shows that SCBV has no obvious sequence similarity and low genetic relatedness to *Badnavirus* and *Tungrovirus* representatives. LSCM studies show that P2 is localized in both the cytoplasm and nucleus. Moreover, P2 is shown to be a suppressor of PTGS and transcriptional gene silencing TGS, which can not only repress ssRNA-induced gene silencing but also disrupt the host RNA-directed DNA methylation (RdDM) pathway. In addition, P2 can trigger an oxidative burst and cause typical hypersensitive-like response (HLR) necrosis in systemic leaves of *N. benthamiana* when expressed by PVX. Overall, our results laid a foundation for deciphering the molecular mechanism of SCBV pathogenesis and made progress for resistance breeding.

# The P2 nucleic acid binding protein of sugarcane bacilliform virus is a viral pathogenic factor

Xiongbiao Xu<sup>1#\*</sup>, Yinian Lou<sup>1#</sup>, Kaili Liang<sup>1</sup>, Jingying Liu<sup>1</sup>, Zhiyuan Wang<sup>1</sup>, Baoshan Chen<sup>1</sup>, Wenlan Li<sup>2</sup>

<sup>1</sup> State Key Laboratory for Conservation and Utilization of Subtropical Agro-bioresources, Guangxi key Laboratory of Sugarcane biology, College of Agriculture, Guangxi University, Nanning, Guangxi, P.R. China

<sup>2</sup> College of Life Science and Technology, Guangxi University, Nanning, Guangxi, P.R. China

\* Corresponding Author:

Xiongbiao Xu<sup>1</sup>

No.100, East Daxue Road, Nanning, Guangxi Province, 530004, P.R. China

Email address: xiongbiaox@gxu.edu.cn

## Abstract

**Background.** *Saccharum spp.* is the major source of sugar and plays significant roles in global renewable bioenergy. Sugarcane bacilliform virus (SCBV) is one of the most important viruses infecting sugarcane, causing severe yield losses and quality degradation. It is of great significance to reveal the pathogenesis of SCBV and resistance breeding. However, little is known about the viral virulence factors or RNA silencing suppressors and the molecular mechanism of pathogenesis.

**Methods.** To systematically investigate the functions of the unknown protein P2 encoded by SCBV ORF2. Phylogenetic analysis was implemented to infer the evolutionary relationship between the P2 of SCBV and other badnaviruses. The precise subcellular localization of P2 was verified in the transient infiltrated *Nicotiana benthamiana* epidermal mesophyll cells and protoplasts by using the Laser scanning confocal microscope (LSCM). The post-transcriptional gene silencing (PTGS) and transcriptional gene silencing (TGS) RNA silencing suppressor activity of P2 was analysed, respectively. And the probable mechanism of P2 on repressing DNA methylation was verified by restriction digestion and RT-qPCR. To explore the pathogenicity of P2, a potato virus X-based viral vector was used to heterologously express SCBV P2, and the consequent H<sub>2</sub>O<sub>2</sub> accumulation was detected by 3,3'-diaminobenzidine (DAB) staining method.

**Results.** Phylogenetic analysis shows that SCBV has no obvious sequence similarity and low genetic relatedness to *Badnavirus* and *Tungrovirus* representatives. LSCM studies show that P2 is localized in both the cytoplasm and nucleus. Moreover, P2 is shown to be a suppressor of PTGS and transcriptional gene silencing TGS, which can not only repress ssRNA-induced gene silencing but also disrupt the host RNA-directed DNA methylation (RdDM) pathway. In addition, P2 can

40 trigger an oxidative burst and cause typical hypersensitive-like response (HLR) necrosis in  
41 systemic leaves of *N. benthamiana* when expressed by PVX. Overall, our results laid a foundation  
42 for deciphering the molecular mechanism of SCBV pathogenesis and made progress for resistance  
43 breeding.

44 **Keywords:** Sugarcane bacilliform virus, phylogenetic relationship, pathogenic factor, RNA  
45 silencing suppressor, hypersensitive-like response.

## 46 Introduction

47 *Saccharum spp.* is a primary sugar-producing crop and an important industrial renewable  
48 bioenergy crop, which is cultivated throughout the world's tropical and subtropical areas.  
49 Sugarcane bacilliform virus (SCBV) is one of the primary viruses infecting sugarcane and causing  
50 severe damage. It was first identified in cultivar B34104 in Cuba in 1985 (Geijskes et al., 2002),  
51 and later purified from cultivar Mex.57-473 (Lockhart, 1988). SCBV is spontaneously spread by  
52 the insect vectors *Dysmicoccus boninsis* and *Saccharicoccus sacchari*. It can also be transmitted  
53 experimentally by raw viral sap or by Agrobacterium-mediated inoculation (Lockhart et al., 1995),  
54 but failed to be transmitted by mechanical friction. In addition, long-distance spread of virus-  
55 infected materials is an important means of transmission. SCBV has a relatively broad host range,  
56 including *Sorghum halepense*, *Brachiaria sp.*, *Rottboellia exaltata*, *Panicum maximum*, and  
57 experimental hosts such as *Oryza sativa* and *Musa sp.* (Bouhida et al., 1993; Lockhart et al., 1995;  
58 Viswanathan et al., 1996). Usually, the visible symptoms caused by SCBV are mottling, stunted  
59 growth, chlorotic streaks, and internode fracture (Viswanathan et al., 1996). Once infection, the  
60 sugarcane plants show varying degrees of reduced juice yield, sugar content, gravity purity and  
61 stem weight, resulting in significant yield and quality losses (Ahmad et al., 2019). Occasionally,  
62 masked symptoms occur due to temperature, drought, nutritional conditions changes. Moreover,  
63 much more complicated symptoms could be found due to co-infection with other viruses (Lockhart  
64 et al., 1995; Singh et al., 2009; Viswanathan and Premachandran, 1998).

65 SCBV belongs to the genus *Badnavirus* (family *Caulimoviridae*), with bacilliform, non-  
66 enveloped virions of 130-150 nm in length and 30 nm in diameter (Bhat et al., 2016; Bouhida et  
67 al., 1993; Lockhart, 1988), containing a circular, covalent, discontinuous dsDNA genome of  
68 approximately 7.5-8.0 kilobases (Kb), which generally encodes three open reading frames (ORFs).  
69 The exact roles of ORF1 and ORF2 have not been confirmed, and ORF3 has been found to encode  
70 a large polyprotein truncated into movement protein (MP), coat protein (CP), aspartic protease  
71 (AP), reverse transcriptase (RT) and ribonuclease H (RNase H), but the precise cutting sites remain  
72 unknown (Geijskes et al., 2002; Sun et al., 2016). Previous studies have suggested that a short  
73 fragment between the 3'-end of ORF3 and ORF1 may act as a strong promoter in both monocot  
74 and dicot species (Davies et al., 2014; Gao et al., 2017). The P2 protein of Corn yellow  
75 mottle virus (CoYMV) has been shown to be involved in virion particle assembly (Cheng et al.,  
76 1996), and the P2 protein encoded by Cacao swollen shoot virus (CSSV) can bind to cognate or  
77 heterologous DNA as well as ssRNA, and the C-terminus appears to be essential for nucleic acid  
78 binding (Jacquot et al., 1996). Jacquot and colleagues have demonstrated that the proline-rich  
79 region (<sub>99</sub>-PPKKGIKRKYP<sub>A-110</sub>) at the C-terminal of Rice tungro bacilliform virus (RTBV) P2


80 plays an important role in the interaction between P2 and nucleic acids (Jacquot et al., 1997). All  
81 these results provide the basis for studying the function of the P2 protein of *Badnavirus*, but little  
82 is known about its roles in viral pathogenicity.


83 In this study, the complete genome of SCBV was deciphered and the functions of its encoded  
84 P2 protein were analyzed. The P2 protein was found to share low sequence similarity with other  
85 badnaviruses and elicit a hypersensitive-like response and suppress posttranscriptional and  
86 transcriptional gene silencing, suggesting that P2 is a viral pathogenicity factor. Our findings  
87 increase our understanding of the pathogenesis of SCBV virus and lay a foundation for antiviral  
88 resistance breeding.

89

## 90 **Materials & Methods**

91 **Source of plant materials.** Sugarcane plants of the Badila cultivar that exhibited mottling,  
92 stunting, and chlorotic streaking symptoms were collected from Menghai County, Yunnan  
93 Province, China, and rapidly frozen in liquid nitrogen and then stored at -80 °C.

94 **Multiple alignment and phylogenetic analyses.** Amino acid sequence similarities were  
95 determined for the P2 of 6 representative members of the genus *Badnavirus* and the sole member  
96 of *Tungrovirus* (Rice tungro cilliform virus, RTBV), all sequences and GenBank accession  
97 numbers are listed in Table 1. Sequence multiple alignment was performed with the MegAlign  
98 program using the DNASTAR software. The corresponding sequences of the above viruses were  
99 aligned, and percent identities were determined in Clustal W. The phylogenetic tree was inferred  
100 via the Neighbor-joining method in MEGA11 with the bootstrap 1, 000 replicates.

101 **Construction of plasmids.** Total genomic DNA was extracted using cetyltrimethylammonium  
102 bromide (CTAB)-based methods as previously described (S nger, 2010). Genomic DNA was  
103 purified after RNase A digestion and used as a template for PCR. The complete genome of SCBV  
104 was obtained by isothermal amplification with Phi29 MAX DNA Polymerase (Cat#: N106-01,  
105 Vazyme, Nanjing, China) according to the manufacturer's instructions. The products of isothermal  
106 amplification were then used as templates for amplification of the complete genome using primer  
107 pair SCBV/F and SCBV/*Sma*I/R (Table S1) and Phanta EVO HS Super-Fidelity DNA Polymerase  
108 (Cat#: P504-d1, Vazyme, Nanjing, China). The SCBV complete genome sequence was then  
109 subcloned into the pCE2-TA/Blunt-Zero vector (Cat#: C601-01, Vazyme, Nanjing, China) and  
110 transformed into *Escherichia coli* Top10. The positive colonies were cultured and verified by PCR  
111 and Sanger sequencing. The complete genome of SCBV was then submitted to National Center  
112 for Biotechnology Information (GenBank accession number: OR672147). The ORF2 coding  
113 sequence was amplified by PCR and cloned into PVX-based vector pGR106 by digested with *Cla*I  
114 and *Sal*I followed by T4 DNA ligase (Cat#: EL0014, ThermoFisher Scientific, Shanghai, China)  
115 ligation to get the recombinant plasmid PVX-P2. Also, P2 was inserted to the pCHF3 binary  
116 expression vector or fused to the N-terminal of enhanced green fluorescent protein (eGFP) in  
117 pCHF3-eGFP by double enzyme digestion with *Sac*I/*Bam*HI,. The corresponding recombinant  
118 plasmids were referred to as pCHF3-P2 and pCHF3-P2-eGFP, respectively. All primers used in  
119 this study are listed in Supplementary Table S1.

120 **Plant growth and agroinoculation.** Wild-type, 16c (Voinnet and Baulcombe, 1997), 16-TGS  
121 (Raja et al., 2008) and RFP-H2B transgenic seedlings of *N. benthamiana* were grown to the 4- to  
122 5-leaf stage in an insect-free chamber at a constant temperature of 25 °C and a 16-h/8-h day/night  
123 cycle. The binary plasmids pCHF3-P2 and empty pCHF3 were transfected into *Agrobacterium*  
124 *tumefaciens* strain EHA105, and the recombinant plasmids PVX and PVX-P2 were transformed  
125 into *A. tumefaciens* GV3101 by electroporation. Suspensions of *A. tumefaciens* cultures were  
126 regulated to OD<sub>600</sub> of 1.0, and the *Agrobacterium* containing PVX-P2 was infiltrated into *N.*  
127 *benthamiana* wild-type or 16-TGS seedlings using a 1-mL syringe without a needle. Transient  
128 PTGS suppression experiments were conducted as previously described (Johansen and Carrington,  
129 2001; Li et al., 2014; Li et al., 2015).

130 **Plant transformation.** The transgenic *N. benthamiana* plants over-expressing P2 or empty vector  
131 were generated by using the *Agrobacterium*-mediated leaf disc transformation method. The binary  
132 empty vector pCHF3 or recombinant plasmid pCHF3-P2 were transformed into *A. tumefaciens*  
133 strain EHA105, and used for transfection of *N. benthamiana* leaf discs. Potential transformants  
134 were selected on MS media containing 200 µg ml<sup>-1</sup> cefotaxime and 200 µg ml<sup>-1</sup> kanamycin.  
135 Kanamycin-resistant cluster buds were cut off, placed on rooting media, cultured to a height of 5-6  
136 cm, and then transplanted into soil. Transgenic seedlings were verified by PCR with CaMV 35S  
137 promoter or P2 specific primers, respectively. Relative levels of P2 mRNA in transgenic plants  
138 were confirmed by RT-qPCR.

139 **H<sub>2</sub>O<sub>2</sub> detection in plants.** H<sub>2</sub>O<sub>2</sub> production was detected visually in *N. benthamiana* leaves using  
140 the 3,3'-diaminobenzidine (DAB) staining method (Cat#: A690009, Sangon Biotech, Shanghai,  
141 China) (Sharma and Ikegami, 2010) and making some modifications as previously described  
142 (Liang et al., 2023).

143 **Subcellular localization analysis.** For subcellular localization experiments, fluorescence in RFP-  
144 H2B transgenic *N. benthamiana* leaf epidermal cells or protoplasts inoculated with pCHF3-eGFP-  
145 and pCHF3-P2-eGFP was examined by confocal microscopy (Leica TCS SP8MP, Mannheim,  
146 Germany) 2- to 3-days post inoculation (dpi) as described (Shen et al., 2011; Yoo et al., 2007).

147 **Protoplast preparation.** To further observe the more precise subcellular localization of SCBV P2  
148 protein, the protoplasts of RFP-H2B transgenic *N. benthamiana* leaf epidermal cells were prepared  
149 by digesting with 1.5% (wt/vol) cellulase (Cat#: A002610, Sangon Biotech, Shanghai, China) and  
150 0.4% (wt/vol) macerozyme R10 (Cat#: A004297, Sangon Biotech, Shanghai, China) as described  
151 (Yoo et al., 2007).

152 **DNA methylation analysis by restriction digestion.** Genomic DNA of pCHF3 and P2 transgenic  
153 plants was extracted by using the CTAB method. Digestion analysis of genomic DNA was  
154 performed by using a methylation-insensitive restriction endonuclease *Bam*HI (Cat#: FD0054,  
155 ThermoFisher Scientific, Shanghai, China) and a methylation-dependent endonuclease *Mcr*BC  
156 (Cat#: M0272, New England Biolabs, Ipswich, MA, USA). The restriction digestion reaction (50  
157 µl) consists of 10 µg of genomic DNA, 50 U of the respective endonuclease according to the  
158 manufacturer's specifications. Digested products were instantly separated by electrophoresis  
159 through a 1.5% agarose gel.



160 **RT-qPCR.** RT-qPCR analysis was performed to measure the transcription level of core genes in  
161 the RNA-directed DNA methylation (RdDM) pathway. Total RNAs from PVX-inoculated *N.*  
162 *benthamiana* and P2 or empty vector-transgenic *N. benthamiana* plants were extracted as  
163 experimental and control groups using RNAiso Plus reagent (Cat#: 9108, Takara, Beijing, China)  
164 and the  $A_{260}/A_{280}$  value and concentration of RNA products were measured by NanoPhotometer®  
165 N60/N50 (IMPLEN, Germany). 2 µg of high-quality RNA were converted to cDNA using HiScript  
166 III 1st Strand cDNA Synthesis Kit (+gDNA wiper) (Cat#: R312-01, Vazyme, Nanjing, China)  
167 according to the manufacturer's instructions. The cDNA product was diluted 10-fold and served  
168 as a template for RT-qPCR. Each reaction mixture contained 2 µL of the diluted cDNA, 10 µL of  
169 2 × ChamQ Universal SYBR qPCR Master Mix (Cat#: Q711-02, Vazyme, Nanjing, China), 0.4  
170 µL of each of the forward and reverse primer (10 µM) in a total volume of 20 µL (primers are  
171 listed in Table S1). Three independent biological and experimental replicates were performed and  
172 the reactions were run under the following program conditions: 95 °C for 30 sec, and 40 cycles of  
173 95 °C for 10 sec and 60 °C for 30 sec. Melting curves were derived (95 °C for 15 sec, 60 °C for 60  
174 sec and 95 °C for 15 sec) for each reaction to ensure a single product. Reactions were performed  
175 using the LightCycler 96 real-time PCR system (F. Hoffmann-La Roche Ltd. Switzerland). The  
176 qPCR data was analyzed by using the  $2^{-\Delta\Delta C_t}$  method (Livak and Schmittgen, 2001). All primers  
177 used for qRT-PCR detection in this study are listed in Supplementary Table S1.

178 **Immunoblotting.** Total protein of systemic leaves was extracted from PVX-infected plants as  
179 described previously (Xiong et al., 2009). Immunoblotting was performed with primary Mouse  
180 anti-PVX CP monoclonal antibodies, followed by HRP-conjugated Goat Anti-Mouse IgG (Cat#:  
181 D110087, Sangon Biotech, Shanghai, China). Blotted membranes were washed thoroughly and  
182 visualized using the SuperPico ECL Chemiluminescence Kit according to the manufacturer's  
183 protocol (Cat#: E422, Vazyme, Nanjing, China).

184

## 185 Results

### 186 Phylogenetic relationships between SCBV P2 and other taxa of the genus Badnavirus

187 The complete genome of SCBV was sequenced and submitted to NCBI (GenBank accession  
188 number: OR672147). The ORF2 of SCBV is 372 nucleotides (nt) long and encodes a small protein  
189 of 123 amino acids (aa) called P2. The complete amino acid sequences of SCBV P2, Rice tungro  
190 bacilliform virus (RTBV, GenBank accession number: AAD30189), and several representative  
191 members of the genus *Badnavirus* (as seen in Table 1) were aligned and phylogenetic analyzed.  
192 Multiple sequence alignment shows that all P2 amino acid sequences have no obvious sequence  
193 similarity (Fig. 1A, Table 1). A coiled-coil-like domain (47-  
194 LLTLHGKITALLEGRLQDLKEDIKKADK-74) was predicted in SCBV P2 by InterPro online  
195 prediction (<https://www.ebi.ac.uk/interpro/>). The coiled-coil like domain is quite conservative in  
196 length and position in all the above viruses (Fig. 1A). Phylogenetic analysis shows that all the 8  
197 viruses were clustered into three groups, and SCBV P2 was assigned in a clade alone and had a  
198 relatively closer relationship with Banana streak OL virus and Cycad leaf necrosis virus P2, and  
199 these three viruses were clustered in the same group (Fig. 1B). We have previously demonstrated

200 that SCBV P2 can bind to both homologous and heterologous nucleic acids in a sequence-  
201 nonspecific manner, and the coiled-coil-like domain plays a major role in P2-nucleic acids binding  
202 through self-interaction (Lou et al., 2023), and this is consistent with that of CSSV and RTBV  
203 (Jacquot et al., 1996; Jacquot et al., 1997). The above results suggest that although the badnaviruses  
204 P2 share little sequence similarity, they all possess a conserved coiled-coil-like domain and play  
205 an indispensable role in P2-nucleic acids affinity binding, and this property is conserved in  
206 badnaviruses and tungroviruses.

### 207 **Subcellular localization of the SCBV P2 protein**

208 To determine the precise subcellular localization of SCBV P2, an enhanced green fluorescent  
209 protein (eGFP) was fused to the C terminus of P2 (P2-eGFP) and subcloned into the binary  
210 expression vector pCHF3 under the transcription of the Cauliflower mosaic virus 35S promoter.  
211 *A. tumefaciens* containing the recombinant plasmid pCHF3-P2-eGFP or the pCHF3-eGFP vector  
212 were infiltrated into 4- to 5-leaf stage RFP-H2B transgenic *N. benthamiana* plants (containing an  
213 RFP nucleus localization signal), respectively. Green fluorescence in inoculum leaves was  
214 observed at 2- to 3-dpi using a confocal microscopy. Fluorescence in plants expressing eGFP alone  
215 (35S-eGFP) was observed in both cytoplasm and nucleus, and fluorescence in P2-eGFP-infiltrated  
216 leaves was also localized in cytoplasm as well as nucleus (Fig. 2A). To further confirm the  
217 subcellular localization of P2, the inoculated leaves were digested with cellulase and macerozyme  
218 to obtain the protoplasts. The eGFP signal of 35S-eGFP infiltrated mesophyll protoplasts was  
219 distributed around the periphery of cytomembrane and nucleus, and it's similar in the 35S-P2-  
220 eGFP infiltrated mesophyll protoplasts except some dense bright fluorescent spot (Fig. 2B) The  
221 above results indicate P2 have a cytoplasm and nucleus subcellular co-localization.

### 222 **RNA silencing suppressor activity of SCBV P2**

223 RNA silencing is an efficient innate antiviral mechanism possessed by plants (Li and Wang, 2019).  
224 To repress the transcription of viral DNAs, host Dicer-like protein directs TGS through RdDM, or  
225 PTGS, which includes splicing and degradation, or translational repression of recognized viral  
226 RNA (Boualem et al., 2016; Matzke and Mosher, 2014). To date, the badnaviruses encoded RNA  
227 silencing suppressor (RSS) has been rarely reported. As we described previously that SCBV P2  
228 can bind both DNA and RNA (Lou et al., 2023) and is localized in both the cytoplasm and nucleus,  
229 suggesting the possibility that it could function as a viral RSS and support viral infection. To test  
230 this hypothesis, we used a 16c-transgenic *N. benthamiana* line as the experimental plant, which  
231 can constitutively express a green fluorescent protein (GFP) signal localized in the endoplasmic  
232 reticulum (ER). *A. tumefaciens* harboring pCHF3-P2 or pCHF3 (negative control) and the p19  
233 suppressor encoded by tomato bushy stunt virus (TBSV) (positive control) was individually mixed  
234 with an equal volume of *A. tumefaciens* containing a recombinant plasmid expressing the RNA  
235 silencing inducer 35S-GFP and inoculated into 4- to 5-leaf aged 16c-transgenic *N. benthamiana*  
236 seedlings. By 4 dpi, the strength of green fluorescence in leaves infiltrated with the pCHF3 empty  
237 vector had decreased dramatically under UV light, and was almost undetectable under stereo  
238 fluorescence microscope, but the intensity remained relatively high in patches expressing P2, and  
239 those inoculated with p19 had the highest fluorescence intensity (Fig. 3A), these data indicate that

240 SCBV P2 is an RSS, which can suppress single stranded RNA (ssRNA) triggered local gene  
241 silencing.

242 To test whether SCBV P2 can suppress dsRNA-induced gene silencing, wild-type *N.*  
243 *benthamiana* plants of 4- to 5-leaf age were infiltrated with *A. tumefaciens* solutions containing  
244 the same volume of transient dsRNA elicitor 35S-GFP and 35S-dsFP together with pCHF3,  
245 pCHF3-P2, and pCHF3-p19, respectively. As shown in Fig. 3B, leaf spots infiltrated with neither  
246 pCHF3 nor pCHF3-P2 mixed with the silencing inducer did not show any GFP fluorescence at 4  
247 dpi under UV light or stereo fluorescence microscopy, indicating that P2 fails to suppress dsRNA-  
248 induced RNA silencing. In contrast, high intensity of green fluorescence was observed in patches  
249 expressing the p19 positive control (Fig. 3B). The above data suggest that SCBV P2 is a weak  
250 local ss-PTGS but not a ds-PTGS suppressor.

251 To determine whether P2 can also conquer TGS, a transgenic *N. benthamiana* line named 16-  
252 TGS (the CaMV 35S promoter of the GFP transgene is transcriptionally silenced) was used.  
253 Transgenic seedlings of 4- to 5-leaf stage were inoculated with GV3101 *A. tumefaciens* solutions  
254 (mock) or PVX-P2, PVX (negative control), or PVX- $\beta$ C1 (the TGS repressor of tomato yellow  
255 leaf curl China betasatellite (TYLCCNB), positive control), respectively. After 21 dpi, PVX-  
256 infected plants were almost asymptomatic and no visible green fluorescence was detected in  
257 systemic tissues under a high intensity UV lamp. However, PVX- $\beta$ C1-infected plants exhibited  
258 severe dwarfing, stem deformation and upward leaf curling along with the PVX-immanent mosaic  
259 symptoms, and GFP fluorescence was quite noticeable. As shown in Fig. 3C, systemic leaves  
260 infected with PVX-P2 showed severe mosaic and spotty mottling symptoms accompanied with  
261 visible green fluorescence under UV light (Fig. 3C), indicating that P2 is a potential TGS repressor.

### 262 **SCBV P2 expression impacts RdDM signaling in the host**

263 In plants, DNA methylation is a conserved epigenetic modification that regulates genome stability,  
264 gene expression, and antiviral defense (He et al., 2022; Wang et al., 2019; Zhang et al., 2018). And  
265 the methylation level of the plant host is reprogrammed when challenged by an invading virus. To  
266 investigate the effect of P2 on the global methylation patterns of the host plant, we constructed a  
267 transgenic P2 line of *N. benthamiana* and tested methylation at the genome level using a  
268 methylcytosine-dependent endonuclease (*McrBC*). Genomic DNA from pCHF3 (Vec) and P2  
269 transgenic *N. benthamiana* plants (5# and 9#) were extracted and subsequently processed with  
270 restriction digestion assays. A mock treatment without enzyme was performed as a control (Sham),  
271 and all genomic DNA samples remained unaltered. When a methylation-insensitive endonuclease  
272 (*BamHI*) was used, we found that all three genomic DNA samples were digested and formed a  
273 'smear' pattern on the agarose gel during electrophoresis (Fig. 4A). However, *McrBC* treatment  
274 cleaved a portion of the Vec DNA, whereas the DNA from the P2 transgenic lines showed high  
275 resistance and remained unchanged (Fig. 4A). The present data suggest that P2 can reduce DNA  
276 methylation on a genome-wide scale when transgenically expressed in *N. benthamiana* plants.

277 To explore the possible mechanism of SCBV P2 in repressing epigenetic TGS and genome-  
278 wide DNA methylation, the relative expression levels of the homologous genes of DNA  
279 methyltransferases, demethylases, histone deacetylase and essential genes related to the RdDM

280 pathway were analyzed in P2 or empty vector transgenic *N. benthamiana* plants. Specific primers  
281 were designed and synthesized for qRT-PCR detection of the homologs of DNA  
282 methyltransferases (MET1, DRM2 and CMT3), demethylases (ROS1, ROS2), argonautes (AGO1-  
283 1, AGO4-1), dicers (DCL3), and histone deacetylase 6 (HDA6). Total RNA from empty vector  
284 (Vec) and P2 transgenic *N. benthamiana* plants was extracted 4 weeks after sowing, and total RNA  
285 from PVX- or PVX-P2-infected *N. benthamiana* plants was isolated at 15 dpi. The above RNA  
286 was reverse transcribed into cDNA and serves as template for the subsequent RT-qPCR assays.  
287 As shown in Fig. 4B and 4C, the expression of *NbAGO1* was significantly down-regulated in both  
288 P2 transgenic plants and PVX-P2-infiltrated plants. and the expression of *NbAGO4* was  
289 dramatically reduced in P2 transgenic *N. benthamiana* plants but remained inconspicuous in PVX-  
290 P2-inoculated plants (Fig. 4B and 4C). Surprisingly, we found that the expression level of  
291 *NbHDA6* was also significantly down-regulated in both P2 transgenic plants and PVX-P2-  
292 infiltrated plants, and HDA6 was proved to be a histone deacetylase and cofactor of MET1 that  
293 promotes DNA methylation. Taken together, our findings show that P2 consistently  
294 overexpression decreases *NbAGO1* and *NbHDA6* expression so as to suppress host TGS.



#### 295 **SCBV P2 induces a hypersensitive-like response (HLR) in *N. benthamiana*.**

296 SCBV infection usually causes pathchy, chlorotic streaking symptoms (Viswanathan et al., 1996),  
297 and induces broken chlorotic streaks in inoculated rice (Bouhida et al., 1993). We successfully  
298 constructed an infectious clone of SCBV by inserting a 1.06 copy of the tandem viral genome into  
299 the binary vector pCB301-2×35S-HDVRZ-NOS (Fig. S1, A and B). After *Agrobacterium*-  
300 mediated inoculation, SCBV-infected rice seedlings showed stunting and broken chlorotic streaks  
301 on leaves at 21 dpi (Fig. S1, C), consistent with the results of Bouhida and colleagues (Bouhida et  
302 al., 1993). We also investigated whether the necrotic streaks were the results of a hypersensitive-  
303 like response. The rice leaves that showed typical necrotic streaks were stained with 3,3'-  
304 diaminobenzidine (DAB), and the mock and pCB301-2×35S-HDVRZ-NOS empty vector  
305 infiltrated plants were used as controls. As shown in Fig. S1, brown necrotic spots appeared in  
306 leaves infected with SCBV, whereas plants inoculated with mock and empty vector remained  
307 transparent and speckless. The accumulation of viral genomic DNA was verified by PCR analysis,  
308 and the results indicate that infectious SCBV can successfully infect rice and cause H<sub>2</sub>O<sub>2</sub>  
309 accumulation-induced HLR.

310 To evaluate whether SCBV P2 is a symptom elicitor in *N. benthamiana*, the P2 protein was  
311 ectopically overexpressed by a PVX-based vector. *N. benthamiana* plants of 4- to 5-leaf stage were  
312 inoculated with *A. tumefaciens* harboring PVX or PVX-P2, respectively. At 7 dpi, PVX-infected  
313 plants began to show typical mosaic and shriveling symptoms, whereas PVX-P2-infiltrated plants  
314 remained symptomless (Fig. 5A, upper panels). At 10 dpi, the symptoms of PVX-P2-infected  
315 plants resembled those of PVX-infected plants (Fig. 5A, middle panels). Symptoms of PVX-  
316 infected plants showed signs of recovery from 12 dpi, and vein chlorosis and mosaic phenotype  
317 disappeared by 20 dpi, whereas P2-expressing plants still exhibited mosaic and leaf wrinkling  
318 phenotypes (Fig. 5A, lower panels). These findings suggest that SCBV P2 can delay the onset of  
319 host symptoms to some extent and persist for a considerably longer period of time. To demonstrate

320 the relationship between necrosis and H<sub>2</sub>O<sub>2</sub> accumulation, the 3,3'-diaminobenzidine (DAB)  
321 staining assay was performed to detect the accumulation of H<sub>2</sub>O<sub>2</sub> in empty or PVX-P2 inoculated  
322 plants at 10 dpi and 20 dpi, and we found that P2-expressing leaves had many brown necrotic spots  
323 at 20 dpi, whereas leaves inoculated with the vector remained spotless (Fig. 5B). Protein  
324 immunoblotting analyses confirmed that PVX CP accumulated in greater amounts in PVX-P2-  
325 inoculated plants than that in PVX-inoculated plants (Fig. 5C), suggesting that P2 is a potential  
326 virulence factor that promotes PVX replication and accumulation. These results indicate that  
327 SCBV P2 protein is a viral pathogenicity factor that can induce a hypersensitive-like response and  
328 promote virus accumulation.

## 329 Discussion

330 Sugarcane  illiform virus (SCBV) is an important member of *Badnavirus* that causes severe  
331 quality and yield loss worldwide. Although many efforts have been made to reveal the molecular  
332 characteristics,  pathogenicity, and pathogenesis of SCBV, little is clear. We previously  
333 demonstrated that the P2 protein of SCBV can bind both viral and heterogenous DNA or RNA in  
334 a sequence nonspecific manner (Lou et al., 2023), which is consistent with the findings of CSSV,  
335 CoYMV, and RTBV (Cheng et al., 1996; Jacquot et al., 1996; Jacquot et al., 1997). Although the  
336 P2 proteins of badnaviruses do not show obvious sequence homology (Fig. 1), they all possess  
337 nucleic acid binding activity, which appears to be a universal property of badnaviruses P2 proteins.  
338 Furthermore, we have proved that the coiled-coil-like region in P2 is critical for self-interaction  
339 and nucleic acid binding (Lou et al., 2023), and the coiled-coil-like region is fairly conserved in  
340 size and position among *Badnavirus* and *Tungrovirus*, indicating its universal crucial role for the  
341 P2 protein. Since P2 has the ability to bind nucleic acids, it could play a key role in preserving  
342 viral nucleic acids from degradation or be involved in virion assembly.

343 RNA silencing is an evolutionarily conserved immune barrier in microbes, such as plant viruses  
344 (Li and Wang, 2019). To overcome this defense, viruses have evolved a variety of proteins (such  
345 as RSSs) capable of suppressing host gene silencing by other PTGS or TGS via the RdDM pathway  
346 (Boualem et al., 2016; Matzke and Mosher, 2014). In general, viral-encoded RSSs are  
347 multifunctional and can play critical roles in various stages of the virus infection in addition to  
348 suppressing RNA silencing (Csorba et al., 2015; Yang and Li, 2018). For example, CaMV P6 has  
349 been proved to act as an RSS by suppressing the activity of DRB4 (Haas et al., 2015). RTBV P4  
350 can inhibit the production of siRNA to suppress RNA silencing (Rajeswaran et al., 2014). Here,  
351 we tested the PTGS repressor activity of SCBV P2 and found that P2 can inhibit sense RNA-  
352 induced but not dsRNA-induced PTGS (Fig. 3), implying that P2 may also repress the formation  
353 of dsRNA or degradation but has no effect on siRNA metabolism. In fact, some other  
354 Caulimovirus-derived suppressor proteins, such as P6 encoded by strawberry vein banding virus  
355 (SVBV), may interfere with dsRNA degradation and act as an RSS (Feng et al., 2018).

356 RdDM is a common epigenetic modification that plays critical roles in gene expression  
357 regulation and defense against invading viruses. As a counter-defense strategy, some plant viruses  
358 encode TGS suppressors as a tactic to block the activity of essential enzymes or protect the  
359 substrates from degradation in the subsequent methylation cycle (Ismayil et al., 2018; Raja et al.,

2008; Yang et al., 2011; Zhang et al., 2011). For example, HC-Pro protein from the *Potyviridae* family is involved in lots of processes of RNA silencing suppression by blocking methylation of the 3'-end of siRNA or directly binding to AGO1 and downregulating its expression, etc. (Valli et al., 2018). And the P0 proteins from the genus *Polerovirus* have been shown to block the binding of siRNAs/miRNAs to the free AGO effector to form an intact RNA-induced silencing complex (RISC) and mediate the degradation of AGO1 via the autophagy pathway (Csorba et al., 2010; Michaeli et al., 2019). In this study, we verified that SCBV P2 inhibits TGS by suppressing the expression of AGO1 and AGO4 (Fig. 4B and 4C), which were known to defend against plant RNA viruses (Morel et al., 2002; Wu et al., 2015; Zhang et al., 2006) and DNA viruses (Raja et al., 2008), respectively. AGO1 regulates gene expression in a variety of developmental and physiological processes (Fei et al., 2013; Rogers and Chen, 2013). It also functions in virus defense when loaded with viral siRNAs via dsRNA-triggered gene silencing (Fang and Qi, 2016; Wu et al., 2015), and in this study P2 downregulate the expression level of *NbAGO1* but had no visible influence on ds-PTGS (Fig. 3 and 4), although the details remain to be elucidated. The AGO4 protein is a crucial component of the RdDM pathway that recruits DRM2, a major de novo methyltransferase, to add methyl to target DNA (Cao and Jacobsen, 2002; Zhong et al., 2014). Furthermore, we found that SCBV P2 transgenic plants showed much lower levels of methylation genome-wide than empty vector transgenic seedlings (Fig. 4A). Taken together, these results provide a model that SCBV P2 represses host DNA methylation by suppressing or disrupting various components involved in the DNA methylation pathway.

Oxidative burst (including  $O_2^-$  and  $H_2O_2$ ) induced HR (Mubin et al., 2010) is universal when plants respond to pathogens and is thought to limit pathogen growth or movement (Hussain et al., 2007; Lam et al., 2001). In this study, we found that SCBV P2 could induce typical mosaic symptoms and HLR necrosis in the late stage of infection with a PVX-based vector (Fig. 5). This suggests that P2 somewhat delays the onset of viral symptoms but triggers  $H_2O_2$  accumulation and causes necrosis symptoms. These results are consistent with the findings of inoculation with infectious clone in *Oryza sativa* (Fig. S1), further confirming that P2 is the pathogenic factor encoded by SCBV. Intriguingly, several plant DNA viruses encoding TGS suppressors have been verified to be virulence factors inducing HR, such as the V2 protein of papaya leaf curl virus (PaLCuV), cotton leaf curl Kokhran virus (CLCuKoV) and tomato leaf curl Java virus (ToLCJV) (Hussain et al., 2007; Mubin et al., 2010; Sharma and Ikegami, 2010). Based on the above results, we suppose that the pathogenesis and TGS repressor activity of SCBV P2 are coupled. Altogether, these observations indicate that SCBV P2 is a multifunctional protein that can suppress PTGS and TGS as well as induce HLR. All these findings help to elucidate the molecular pathogenesis of *Badnavirus* and provide a possible target for future antiviral breeding.

395

## 396 Conclusions

397 Our work reveals the fact that the P2 protein encoded by sugarcane bacilliform virus (SCBV) plays  
398 an important role in the pathogenicity of the virus, which serves as a ss-PTGS suppressor and  
399 represses host TGS by impairing host genome wide DNA methylation level and inhibiting core

400 genes transcription in RdDM pathway, such as AGO1. Besides, P2 was proved to be a virulence  
401 factor, which can induce HLR and assist PVX accumulation in *N. benthamiana*. Our conclusions  
402 increase the awareness of the molecular mechanism of pathogenesis, as well as help lay a  
403 foundation for disease resistance breeding.

404

### 405 **Acknowledgements**

406 We thank professor Xueping Zhou from Institute of Plant Protection, Chinese Academy of  
407 Agricultural Sciences for kindly giving the PVX-based expression vector and Mouse anti-PVX CP  
408 monoclonal antibody. And we also thank professor Xiaorong Tao from Nanjing Agriculture  
409 University for kindly providing the pCB301-2×35S-HDVRZ-NOS binary vector.

410

### 411 **Additional information and declarations**

412

### 413 **Funding**

414 This research was supported by the Natural Science Foundation of Guangxi Province  
415 (2023GXNSFBA026058), the Sugarcane Research Foundation of Guangxi University  
416 (2022GZB011) and the Innovation Project of Guangxi Graduate Education (YCSW2022065).

417

### 418 **Grant disclosures**

419 The following grant information was disclosed by the authors:  
420 Natural Science Foundation of Guangxi Province: 2023GXNSFBA026058.  
421 Sugarcane Research Foundation of Guangxi University: 2022GZB011.  
422 Innovation Project of Guangxi Graduate Education: YCSW2022065.

### 423 **Competing interests**

424 The authors declare there are no competing interests.

### 425 **Author contributions**

426 Yinian Lou analyzed the data, performed the experiments, prepared figures and/or tables, wrote  
427 drafts of the paper, and approved the final draft.

428 Kaili Liang, Jingying Liu and Zhiyuan Wang analyzed the data, performed the experiments,  
429 prepared figures and/or tables.

430 Baoshan Chen and Wenlan Li reviewed and revised drafts of the paper.

431 Xiongbiao Xu conceived and designed the experiments, authored or reviewed drafts of the paper,  
432 and approved the final draft.

433

434

### 435 **References**

- 436 Ahmad K, Sun SR, Chen JL, Huang MT, Fu HY, Gao SJ. 2019. Presence of diverse sugarcane  
437 bacilliform viruses infecting sugarcane in China revealed by pairwise sequence comparisons  
438 and phylogenetic analysis. *Plant Pathology Journal* 35(1): 41-50. doi:  
439 10.5423/PPJ.OA.08.2018.0156.
- 440 Bhat AI, Hohn T, Selvarajan R. 2016. Badnaviruses: The Current Global Scenario. *Viruses*  
441 8(6):177. doi: 10.3390/v8060177.
- 442 Boualem A, Dogimont C, Bendahmane A. 2016. The battle for survival between viruses and their  
443 host plants. *Current Opinion in Virology* 17: 32-38. doi: 10.1016/j.coviro.2015.12.001.
- 444 Bouhida M, Lockhart BE, Olszewski NE. 1993. An analysis of the complete sequence of a  
445 sugarcane bacilliform virus genome infectious to banana and rice. *Journal of General*  
446 *Virology* 74 (Pt 1): 15-22. doi: 10.1099/0022-1317-74-1-15.
- 447 Cao X, Jacobsen SE. 2002. Role of the arabidopsis DRM methyltransferases in de novo DNA  
448 methylation and gene silencing. *Current Biology* 12(13):1138-1144. doi: 10.1016/s0960-  
449 9822(02)00925-9.
- 450 Cheng CP, Lockhart BE, Olszewski NE. 1996. The ORF I and II proteins of Commelina yellow  
451 mottle virus are virion-associated. *Virology* 223(2): 263-271. doi: 10.1006/viro.1996.0478.
- 452 Csorba T, Kontra L, Burgyán J. 2015. viral silencing suppressors: Tools forged to fine-tune host-  
453 pathogen coexistence. *Virology* 479-480: 85-103. doi: 10.1016/j.virol.2015.02.028.
- 454 Csorba T, Lózsza R, Hutvágner G, Burgyán J. 2010. Polerovirus protein P0 prevents the assembly  
455 of small RNA-containing RISC complexes and leads to degradation of ARGONAUTE1.  
456 *Plant Journal* 62(3): 463-472. doi: 10.1111/j.1365-313X.2010.04163.x.
- 457 Davies JP, Reddy V, Liu XL, Reddy AS, Ainley WM, Thompson M, Sastry-Dent L, Cao Z,  
458 Connell J, Gonzalez DO, Wagner DR. 2014. Identification and use of the sugarcane  
459 bacilliform virus enhancer in transgenic maize. *BMC Plant Biology* 14: 359. doi:  
460 10.1186/s12870-014-0359-3.
- 461 Fang X, Qi Y. 2016. RNAi in Plants: An Argonaute-Centered View. *Plant Cell* 28(2): 272-285.  
462 doi: 10.1105/tpc.15.00920.
- 463 Fei Q, Xia R, Meyers BC. 2013. Phased, secondary, small interfering RNAs in posttranscriptional  
464 regulatory networks. *Plant Cell* 25(7): 2400-2415. doi: 10.1105/tpc.113.114652.
- 465 Feng M, Zuo D, Jiang X, Li S, Chen J, Jiang L, Zhou X, Jiang T. 2018. Identification of Strawberry  
466 vein banding virus encoded P6 as an RNA silencing suppressor. *Virology* 520: 103-110. doi:  
467 10.1016/j.virol.2018.05.003.
- 468 Gao SJ, Damaj MB, Park JW, Wu XB, Sun SR, Chen RK, Mirkov TE. 2017. A novel Sugarcane  
469 bacilliform virus promoter confers gene expression preferentially in the vascular bundle and  
470 storage parenchyma of the sugarcane culm. *Biotechnology for Biofuels* 10: 172. doi:  
471 10.1186/s13068-017-0850-9.
- 472 Geijskes RJ, Braithwaite KS, Dale JL, Harding RM, Smith GR. 2002. Sequence analysis of an  
473 Australian isolate of sugarcane bacilliform badnavirus. *Archives of Virology* 147(12):2393-  
474 404. doi: 10.1007/s00705-002-0879-2.



- 475 Haas G, Azevedo J, Moissiard G, Geldreich A, Himber C, Bureau M, Fukuhara T, Keller M,  
476 Voinnet O. 2015. Nuclear import of CaMV P6 is required for infection and suppression of  
477 the RNA silencing factor DRB4. *EMBO Journal* 27(15):2102-2112. doi:  
478 10.1038/emboj.2008.129.
- 479 He L, Huang H, Bradai M, Zhao C, You Y, Ma J, Zhao L, Lozano-Duran R, Zhu JK. 2022. DNA  
480 methylation-free Arabidopsis reveals crucial roles of DNA methylation in regulating gene  
481 expression and development. *Nature Communications* 13(1): 1335. doi: 10.1038/s41467-  
482 022-28940-2.
- 483 Hussain M, Mansoor S, Iram S, Zafar Y, Briddon RW. 2007. The hypersensitive response to  
484 tomato leaf curl New Delhi virus nuclear shuttle protein is inhibited by transcriptional  
485 activator protein. *Molecular Plant-Microbe Interactions* 20(12): 1581-1588. doi:  
486 10.1094/MPMI-20-12-1581.
- 487 Ismayil A, Haxim Y, Wang Y, Li H, Qian L, Han T, Chen T, Jia Q, Yihao Liu A, Zhu S, Deng H,  
488 Gorovits R, Hong Y, Hanley-Bowdoin L, Liu Y. 2018. Cotton leaf curl Multan virus C4  
489 protein suppresses both transcriptional and post-transcriptional gene silencing by interacting  
490 with SAM synthetase. *PLoS Pathogens* 14(8): e1007282. doi: 10.1371/journal.ppat.1007282.
- 491 Jacquot E, Hagen LS, Jacquemond M, Yot P. 1996. The open reading frame 2 product of cacao  
492 swollen shoot badnavirus is a nucleic acid-binding protein. *Virology* 225(1): 191-195. doi:  
493 10.1006/viro.1996.0587.
- 494 Jacquot E, Keller M, Yot P. 1997. A short basic domain supports a nucleic acid-binding activity  
495 in the rice tungro bacilliform virus open reading frame 2 product. *Virology* 239(2): 352-359.  
496 doi: 10.1006/viro.1997.8859.
- 497 Johansen LK, Carrington JC. 2001. Silencing on the spot. Induction and suppression of RNA  
498 silencing in the Agrobacterium-mediated transient expression system. *Plant Physiology*  
499 126(3), 930-938. doi: 10.1104/pp.126.3.930.
- 500 Lam E, Kato N, Lawton M. 2001. Programmed cell death, mitochondria and the plant  
501 hypersensitive response. *Nature* 411(6839): 848-853. doi: 10.1038/35081184.
- 502 Li F, Huang C, Li Z, Zhou X. 2014. Suppression of RNA silencing by a plant DNA virus satellite  
503 requires a host calmodulin-like protein to repress RDR6 expression. *PLoS Pathogens* 10(2):  
504 e1003921. doi: 10.1371/journal.ppat.1003921.
- 505 Li F, Wang A. 2019. RNA-Targeted Antiviral Immunity: More Than Just RNA Silencing. *Trends*  
506 *in Microbiology* 27 (9):792-805. doi: 10.1016/j.tim.2019.05.007.
- 507 Li F, Xu X, Huang C, Gu Z, Cao L, Hu T, Ding M, Li Z, Zhou X. 2015. The AC5 protein encoded  
508 by Mungbean yellow mosaic India virus is a pathogenicity determinant that suppresses RNA  
509 silencing-based antiviral defenses. *New Phytologist* 208(2): 555-569. doi:  
510 10.1111/nph.13473.
- 511 Liang K, Liu J, Bao Y, Wang Z, Xu X. 2023. Screening and identification of host factors interacting  
512 with the virulence factor P0 encoded by Sugarcane yellow leaf virus by Yeast two-hybrid  
513 assay. *Genes* 14(7): 1397. doi: 10.3390/genes14071397.

- 514 Livak KJ, Schmittgen TD. 2001. Analysis of relative gene expression data using real-time  
515 quantitative PCR and the 2(-Delta Delta C(T)) Method. *Methods* 25(4):402-408. doi:  
516 10.1006/meth.2001.1262.
- 517 Lockhart BEL, Irey MJ, Comstock JC. 1995. Sugarcane bacilliform virus, Sugarcane mild mosaic  
518 virus and Sugarcane yellow leaf syndrome, Sugarcane Germplasm Conservation &  
519 Exchange: Report of An International Workshop Held in Brisbane.
- 520 Lockhart BEL. 1988. Occurrence in sugarcane of a bacilliform virus related serologically to  
521 banana streak virus. *Plant Disease* 72(3): 230-233. doi:10.1094/PD-72-0230.
- 522 Lou Y, Liang K, Liu J, Wang Z, Xu X. 2023. Nucleic acid binding activity analysis and key domain  
523 identification of Sugarcane bacilliform virus encoded P2 protein. *Genomics and Applied*  
524 *Biology* (in Chinese). <http://kns.cnki.net/kcms/detail/45.1369.Q.20230314.1511.002.html>.
- 525 Matzke MA, Mosher RA. 2014. RNA-directed DNA methylation: an epigenetic pathway of  
526 increasing complexity. *Nature Reviews Genetics* 15(6): 394-408. doi: 10.1038/nrg3683.
- 527 Michaeli S, Clavel M, Lechner E, Viotti C, Wu J, Dubois M, Hacquard T, Derrien B, Izquierdo E,  
528 Lecorbeiller M, Bouteiller N, De Cilia J, Ziegler-Graff V, Vaucheret H, Galili G, Genschik  
529 P. 2019. The viral F-box protein P0 induces an ER-derived autophagy degradation pathway  
530 for the clearance of membrane-bound AGO1. *Proceedings of the National Academy of*  
531 *Science of the United States of America* 116(45): 22872-22883. doi:  
532 10.1073/pnas.1912222116.
- 533 Morel JB, Godon C, Mourrain P, Béclin C, Boutet S, Feuerbach F, Proux F, Vaucheret H. 2002.  
534 Fertile hypomorphic ARGONAUTE (ago1) mutants impaired in post-transcriptional gene  
535 silencing and virus resistance. *Plant Cell* 14(3): 629-639. doi: 10.1105/tpc.010358.
- 536 Mubin M, Amin I, Amrao L, Briddon RW, Mansoor S. 2010. The hypersensitive response induced  
537 by the V2 protein of a monopartite begomovirus is countered by the C2 protein. *Molecular*  
538 *Plant Pathology* 11(2): 245-254. doi: 10.1111/j.1364-3703.2009.00601.x.
- 539 Raja P, Sanville BC, Buchmann RC, Bisaro DM. 2008. Viral genome methylation as an epigenetic  
540 defense against geminiviruses. *Journal of Virology* 82(18): 8997-9007. Viral genome  
541 methylation as an epigenetic defense against geminiviruses
- 542 Rajeswaran R, Golyaev V, Seguin J, Zvereva AS, Farinelli L, Pooggin MM. 2014. Interactions of  
543 Rice tungro bacilliform pararetrovirus and its protein P4 with plant RNA-silencing  
544 machinery. *Molecular Plant-Microbe Interactions* 27(12): 1370-1378. doi: 10.1094/MPMI-  
545 07-14-0201-R.
- 546 Rogers K, Chen X. 2013. Biogenesis, turnover, and mode of action of plant microRNAs. *Plant*  
547 *Cell* 25(7): 2383-2399. doi: 10.1105/tpc.113.113159.
- 548 Sharma P, Ikegami M. 2010. Tomato leaf curl Java virus V2 protein is a determinant of virulence,  
549 hypersensitive response and suppression of posttranscriptional gene silencing. *Virology*  
550 396(1): 85-93. doi: 10.1016/j.virol.2009.10.012.
- 551 Shen Q, Liu Z, Song F, Xie Q, Hanley-Bowdoin L, Zhou X. 2011. Tomato SlSnRK1 Protein  
552 Interacts with and Phosphorylates  $\beta$ C1, a Pathogenesis Protein Encoded by a Geminivirus  $\beta$ -  
553 Satellite. *Plant Physiology* 157(3): 1394-1406. doi: 10.1104/pp.111.184648.

- 554 Singh D, Tewari AK, Rao GP, Karuppaiah R, Viswanathan R, Arya M, Baranwal VK. 2009. RT-  
555 PCR/PCR analysis detected mixed infection of DNA and RNA viruses infecting sugarcane  
556 crops in different states of India. *Sugar Tech* 11(4): 373-380. doi:10.1007/s12355-009-0064-  
557 y.
- 558 Springer NM. 2010. Isolation of plant DNA for PCR and genotyping using organic extraction and  
559 CTAB. *Cold Spring Harbor Protocols*. 2010(11):pdb.prot5515. doi: 10.1101/pdb.prot5515.
- 560 Sun SR, Damaj MB, Alabi OJ, Wu XB, Mirkov TE, Fu HY, Chen RK, Gao SJ. 2016. Molecular  
561 characterization of two divergent variants of sugarcane bacilliform viruses infecting  
562 sugarcane in China. *European Journal of Plant Pathology* 145(2):375-384.  
563 doi:10.1007/s10658-015-0851-0.
- 564 Valli AA, Gallo A, Rodamilans B, Lopez-Moya JJ, Garcia JA. 2018. The HCPro from the  
565 Potyviridae family: an enviable multitasking Helper Component that every virus would like  
566 to have. *Molecular Plant Pathology* 19(3): 744-763. doi: 10.1111/mpp.12553.
- 567 Viswanathan R, Alexander KC, Garg ID. 1996. Detection of sugarcane bacilliform virus in  
568 sugarcane germplasm. *Acta Virologica* 40(1): 5-8.
- 569 Viswanathan R, Premachandran MN. 1998. Occurrence and distribution of sugarcane bacilliform  
570 virus in the sugarcane germplasm collection in India. *Sugar Cane (United Kingdom)*.
- 571 Voinnet O, Baulcombe DC. 1997. Systemic signalling in gene silencing. *Nature* 389(6651): 553.  
572 doi: 10.1038/39215.
- 573 Wang C, Wang C, Zou J, Yang Y, Li Z, Zhu S. 2019. Epigenetics in the plant-virus interaction.  
574 *Plant Cell Reports* 38(9): 1031-1038. doi: 10.1007/s00299-019-02414-0.
- 575 Wu J, Yang Z, Wang Y, Zheng L, Ye R, Ji Y, Zhao S, Ji S, Liu R, Xu L, Zheng H, Zhou Y, Zhang  
576 X, Cao X, Xie L, Wu Z, Qi Y, Li Y. 2015. Viral-inducible Argonaute18 confers broad-  
577 spectrum virus resistance in rice by sequestering a host microRNA. *eLife* 4, e05733. doi:  
578 10.7554/eLife.05733.
- 579 Xiong R, Wu J, Zhou Y, Zhou X. 2009. Characterization and subcellular localization of an RNA  
580 silencing suppressor encoded by Rice stripe tenuivirus. *Virology* 387(1):29-40. doi:  
581 10.1016/j.virol.2009.01.045.
- 582 Yang X, Xie Y, Raja P, Li S, Wolf JN, Shen Q, Bisaro DM, Zhou X. 2011. Suppression of  
583 methylation-mediated transcriptional gene silencing by  $\beta$ C1-SAHH protein interaction during  
584 geminivirus-betasatellite infection. *PLoS Pathogens* 7(10): e1002329. doi:  
585 10.1371/journal.ppat.1002329.
- 586 Yang Z, Li Y. 2018. Dissection of RNAi-based antiviral immunity in plants. *Current Opinion in*  
587 *Virology* 32: 88-99. doi: 10.1016/j.coviro.2018.08.003.
- 588 Yoo SD, Cho YH, Sheen J. 2007. Arabidopsis mesophyll protoplasts: a versatile cell system for  
589 transient gene expression analysis. *Nature Protocols* 2(7): 1565-1572. doi:  
590 10.1038/nprot.2007.199.
- 591 Zhang H, Lang Z, Zhu JK. 2018. Dynamics and function of DNA methylation in plants. *Nature*  
592 *Reviews Molecular Cell Biology* 19(8): 489-506. doi: 10.1038/s41580-018-0016-z.

- 593 Zhang X, Yuan YR, Pei Y, Lin SS, Tuschl T, Patel DJ, Chua NH. 2006. Cucumber mosaic virus-  
594 encoded 2b suppressor inhibits Arabidopsis Argonaute1 cleavage activity to counter plant  
595 defense. *Genes & Development* 20(23): 3255-3268. doi: 10.1101/gad.1495506.
- 596 Zhang Z, Chen H, Huang X, Xia R, Zhao Q, Lai J, Teng K, Li Y, Liang L, Du Q, Zhou X, Guo H,  
597 Xie Q. 2011. BSCTV C2 attenuates the degradation of SAMDC1 to suppress DNA  
598 methylation-mediated gene silencing in Arabidopsis. *Plant Cell* 23(1): 273-288. doi:  
599 10.1105/tpc.110.081695.
- 600 Zhong X, Du J, Hale CJ, Gallego-Bartolome J, Feng S, Vashisht AA, Chory J, Wohlschlegel JA,  
601 Patel DJ, Jacobsen SE. 2014. Molecular mechanism of action of plant DRM de novo DNA  
602 methyltransferases. *Cell* 157(5): 1050-1060. doi: 10.1016/j.cell.2014.03.056.
- 603
- 604

**Table 1** (on next page)

Amino acid sequences of P2 from sugarcane bacilliform virus (SCBV) and representatives within genus *Badnavirus* and *Tungrovirus*

<sup>a</sup> BSOLV, Banana streak OL virus; CLNV, Cycad leaf necrosis virus; CoYMV, Commelina yellow mottle virus; CSSV, Cacao swollen shoot virus; PYMoV, Piper yellow mottle virus; RTBV, Rice tungro bacilliform virus; SCBV, Sugarcane bacilliform virus; TaBCHV, Taro bacilliform CH virus.

## TABLES

**TABLE 1.** Amino acid sequences of P2 from sugarcane bacilliform virus (SCBV) and representatives within genus *Badnavirus* and *Tungrovirus*

<b>Virus <sup>a</sup></b>	<b>Genus</b>	<b>GenBank accession number</b>	<b>Size (aa)</b>	<b>Amino acid sequence identity (%)</b>
<b>SCBV</b>	<i>Badnavirus</i>	WON00947	123	-
<b>BSOLV</b>	<i>Badnavirus</i>	NP_569149	135	26.8
<b>CLNV</b>	<i>Badnavirus</i>	YP_002117530	128	31.1
<b>CoYMV</b>	<i>Badnavirus</i>	NP_039819	136	19.5
<b>CSSV</b>	<i>Badnavirus</i>	NP_041733	133	24.6
<b>PYMoV</b>	<i>Badnavirus</i>	AXG50781	159	23.8
<b>TaBCHV</b>	<i>Badnavirus</i>	YP_009130663	126	28.3
<b>RTBV</b>	<i>Tungrovirus</i>	AAD30189	111	22.9

<sup>a</sup> BSOLV, Banana streak OL virus; CLNV, Cycad leaf necrosis virus; CoYMV, Commelina yellow mottle virus; CSSV, Cacao swollen shoot virus; PYMoV, Piper yellow mottle virus; RTBV, Rice tungro bacilliform virus; SCBV, Sugarcane bacilliform virus; TaBCHV, Taro bacilliform CH virus.

# Figure 1

Figure 1. Phylogenetic relationships between SCBV and other taxa in the genus *Badnavirus* and *Tungrovirus*.

(A) Multiple alignment of amino acid sequence of SCBV P2 and representatives of *Badnavirus* and *Tungrovirus*. The conserved motifs were highlighted and the coiled coil like domain were framed in a rectangle. (B) Unrooted neighbor-joining phylogenetic tree reconstructed from the alignment of the amino acid sequences of SCBV P2 and other taxa in the genus *Badnavirus* and *Tungrovirus*. The phylogenetic tree was constructed by using the MEGA7.0 program and the percentage of bootstrap values (1,000 replicates) are shown at the branch internodes. BSOLV, Banana streak OL virus; CLNV, Cycad leaf necrosis virus; CoYMV, Commelina yellow mottle virus; CSSV, Cacao swollen shoot virus; PYMoV, Piper yellow mottle virus; RTBV, Rice tungro bacilliform virus; SCBV, Sugarcane bacilliform virus; TaBCHV, Taro bacilliform CH virus.

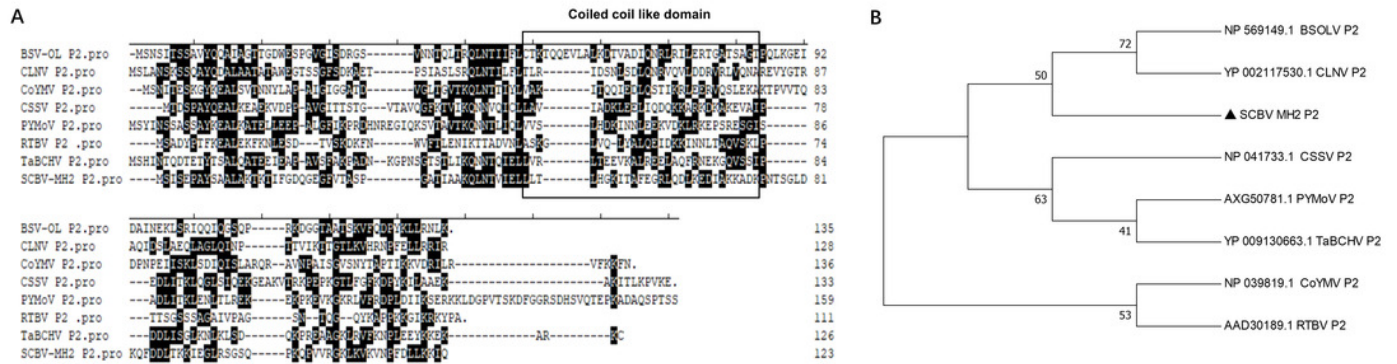




## Figure 2

Figure 2. Subcellular localization of SCBV P2 in RFP-H2B transgenic *Nicotiana benthamiana* mesophyll cells and protoplasts.

(A) Subcellular localization of P2 fused to the enhanced green fluorescent protein (eGFP) in RFP-H2B transgenic *N. benthamiana* mesophyll cells. (B) Subcellular localization of P2 fused to eGFP in RFP-H2B transgenic *N. benthamiana* protoplasts. The 35S-eGFP expression plasmid was used as a control. The ratio scale was shown in the bottom right corner of the picture.

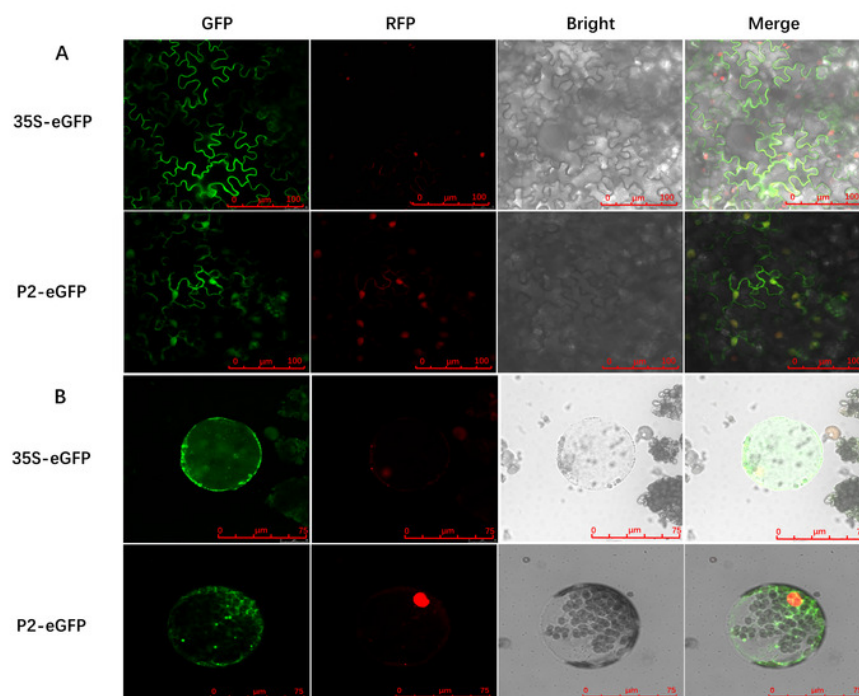


## Figure 3

Figure 3. SCBV P2 inhibits ssRNA induced PTGS and reverses TGS.

(A) Repression of GFP silencing in *N. benthamiana* 16c leaves. Leaf areas were co-infiltrated with *A. tumefaciens* expressing GFP (35S-GFP) and either a pCHF3 control, SCBV P2 (pCHF3-SCBV-P2), or TBSV p19 (pCHF3-p19). Photos of the above infiltrated leaves were taken at 4 dpi, under high intensity UV light. (B) Leaf patches of *N. benthamiana* were co-infiltrated with *A. tumefaciens* carrying GFP (35S-GFP) and dsFP (35S-dsFP), as well as pCHF3 vector, SCBV P2 or p19, and typical leaf patches were photographed under high intensity UV light at 4 dpi. (C) Plant of *N. benthamiana* 16-TGS were left uninoculated, or inoculated with PVX, PVX-P2, or PVX- $\beta$  C1, respectively, and the apex of plants and leaves were photographed under high intensity UV light at 21 dpi.

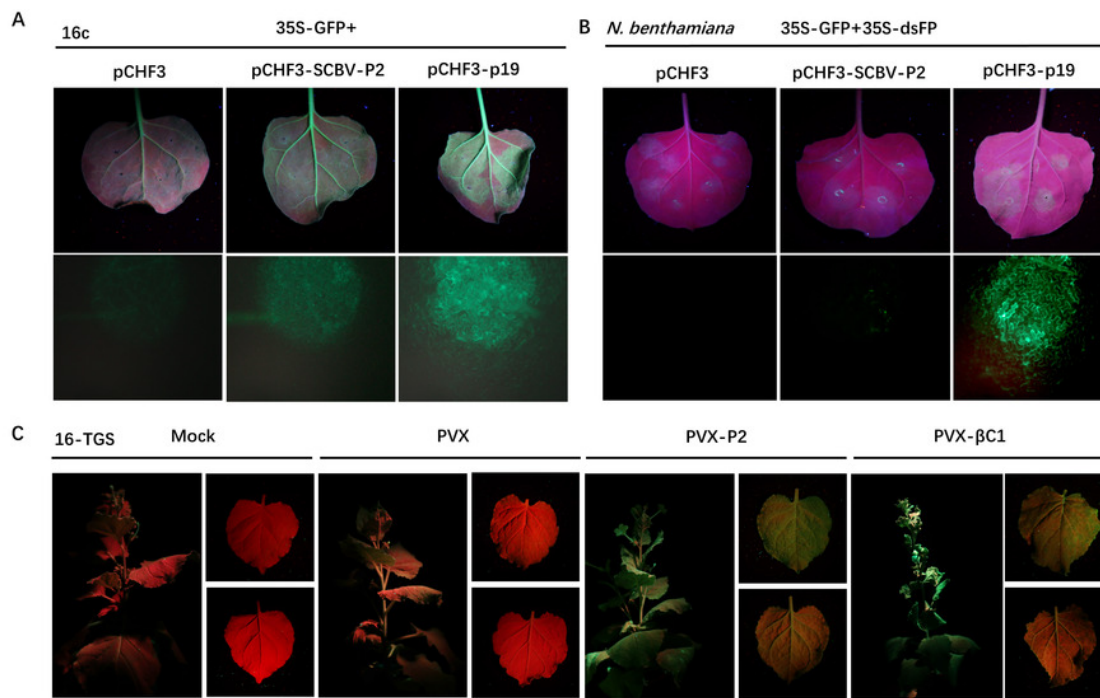


## Figure 4

Figure 4. SCBV P2 expression impacts host RdDM pathway and genome-wide scale methylation.

(A) DNA methylation analysis in P2 transgenic *N. benthamiana* plants using restriction endonuclease digestion. The methylation-dependent endonuclease *McrBC* and the methylation-insensitive enzyme *BamHI* were used to digest genomic DNA isolated from the vector control (Vec) and two separate lines of P2 transgenic plants (5# and 9#). The term 'Sham' refers to a simulated digestion that contains no enzyme. The positions of the uncut input and the digested products are shown. (B) SCBV P2 Overexpression inhibits transcription of *N. benthamiana* ARGONAUTE 1 (*NbAGO1*) and *NbAGO4* in PVX-treated plants. RT-qPCR assays were performed to analyze the effects of P2 on the expression of homologous genes of DNA methyltransferases, demethylases, histone deacetylase and essential genes related to RdDM. Relative expression levels of DNA METHYLTRANSFERASE1 (*NbMET1*) [GenBank accession number: FJ222441], DOMAINS REARRANGED METHYLTRANSFERASE2 (*NbDRM2*) (JQ957857), CHROMOMETHYLASE3 (*NbCMT3*) (JQ957858), DICER3 (*NbDCL3*) (FM986782), REPRESSOR OF SILENCING 1 (*NbROS1*) (JQ957859), *NbROS2* (JQ957860), *NbAGO1* (DQ321488), *NbAGO4* (DQ321490) and Histone Deacetylase 6 (*NbHDA6*) (KU170188) were measured in PVX and PVX-P2 inoculated *N. benthamiana* plants at 15 dpi (B), or in pCHF3 vector and P2 transgenic plants at 30 days after sprouting [C]. T-tests were performed to analyze the significance of difference (\* $P < 0.05$ , \*\* $P < 0.01$ ). Each of the experiments were carried out at least three times.

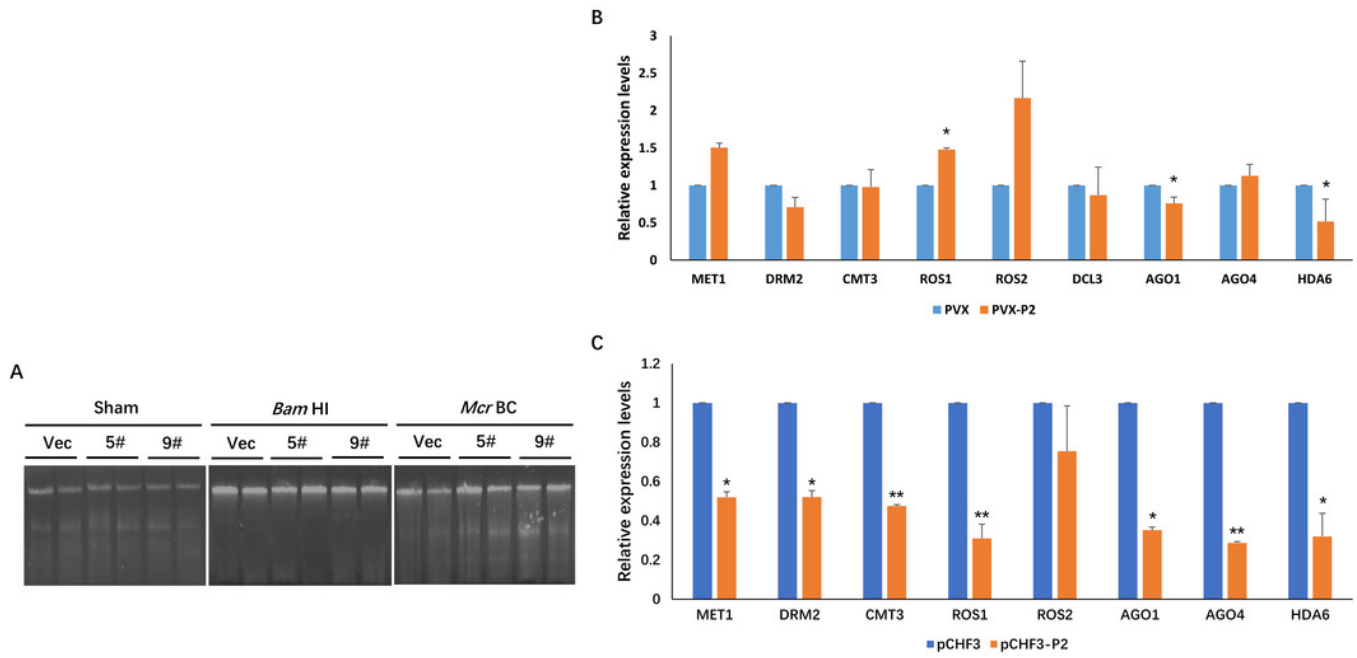


## Figure 5

Figure 5. Symptoms of the plants inoculated with Potato virus X(PVX) or PVX-P2.

(A) Symptoms evoked on *N. benthamiana* plants at 7-, 10- and 20-dpi inoculated with PVX or PVX-P2. (B) PVX-P2 induced mosaic symptoms and necrotic spots on *N. benthamiana* plants. Upper systemic leaves were photographed at 10- and 20-dpi, respectively. Followed by photographing after 3,3'-diaminobenzidine (DAB) treatment. The necrotic lesions are shown by the red arrowheads. (C) Western blot analysis of coat protein (CP) accumulation in PVX or PVX-P2 infected plants. Freshly emerging leaves were used to extract total protein. The anti-PVX CP monoclonal antibody was used to detect the accumulation of PVX, Coomassie light blue stained Rubisco large subunit protein was used as a loading control. The gray values of the blot bands were evaluated by using the ImageJ software, the relative amount of CP accumulation in PVX-infected plants was preset as 100%.

